# Microscopic Description of 800-MeV Polarized-Proton Scattering from $^{16}O$

G. S. Adams, Th. S. Bauer,[a] G. Igo, G. Pauletta, C. A. Whitten, Jr., and A. Wriekat
*Physics Department, University of California, Los Angeles, California 90024*

and

G. W. Hoffmann
*Physics Department, University of Texas, Austin, Texas 78712, and Los Alamos Scientific Laboratory, Los Alamos, New Mexico 87545*

and

G. R. Smith
*Physics Department, University of Colorado, Boulder, Colorado 80302*

and

M. Gazzaly[b]
*Physics Department, University of Pennsylvania, Philadelphia, Pennsylvania 19104*

and

L. Ray
*Los Alamos Scientific Laboratory, Los Alamos, New Mexico 87545*

and

W. G. Love
*Department of Physics and Astronomy, University of Georgia, Athens, Georgia 30602*

and

F. Petrovich
*Physics Department, Florida State University, Tallahassee, Florida 32306*
(Received 30 April 1979)

Differential cross sections and analyzing powers have been measured for elastic and inelastic scattering of 800-MeV protons by $^{16}O$. Microscopic analyses utilizing the impulse approximation are used to study the ground-state neutron distribution of $^{16}O$, and to demonstrate the importance of the spin-orbit amplitudes for the inelastic transitions.

In this Letter we present new differential-cross-section and analyzing-power data for the elastic and inelastic scattering of 800-MeV transversely polarized protons from $^{16}O$. The results of microscopic impulse-approximation calculations are compared with the data. The approach followed is that of Kerman, McManus, and Thaler (KMT).[1] Although several impulse-approximation analyses of elastic and inelastic proton-nucleus scattering data have been recently reported in the literature, (e.g., see Refs. 2–5), these are not subject to the additional constraints provided by measurements of the inelastic analyzing power. The forward-angle analyzing powers for the inelastic transitions are a direct reflection of the spin-orbit amplitudes.

Data were obtained with use of the high-resolution spectrometer at the Clinton P. Anderson Meson Physics Facility (LAMPF). The data, shown in Figs. 1 and 2, include elastic scattering from 6° to 26° (c.m.) and angular distributions for exciting the lowest $J^\pi = 1^-$(7.12 MeV), $2^+$(6.92 MeV), $3^-$(6.13 MeV), and $2^-$(8.87 MeV) states. Differential cross sections were normalized to the known $p+p$ cross section[6] at 30° (lab) by utilizing the hydrogen present in the 64-mg/cm$^2$ Mylar target, resulting in a ±15% normalization uncertainty. The beam energy was determined to be 800±2 MeV, based on the kinematic energy shift between elastic scattering from $^{16}O$ and $^{40}Ca$. The beam polarization (typically 75%) was continuously monitored with a hydrogen polarimeter,[7] located upstream from the target. The $^{12}C$ present in the Mylar target limited the useful excitation range in $^{16}O$ to less than 9 MeV. Overall energy resolution for these data was 130–190 keV full width at half maximum (FWHM) (sufficient to resolve the $1^-$ state from the $2^+$ at most angles). At a few angles where $^{12}C$ peaks overlapped $^{16}O$ excited states, data from a water target were

 

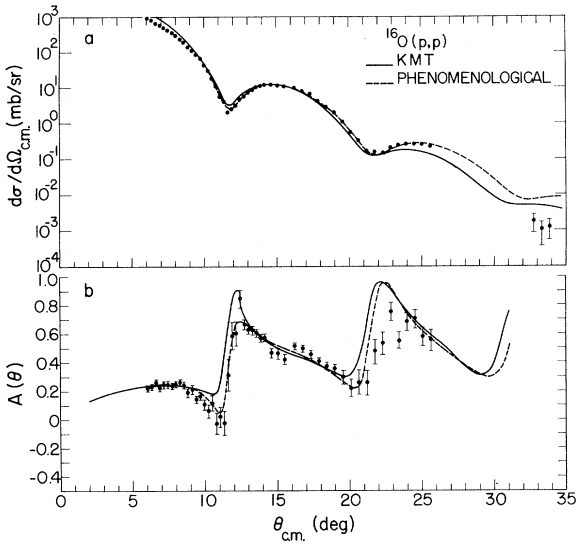


FIG. 1. Differential cross sections and analyzing powers for elastic scattering. Statistical errors are smaller than the data points unless otherwise indicated.

acquired with a resolution of about 300 keV FWHM.

The elastic scattering data have been analyzed using optical potentials generated both phenomenologically and with the microscopic KMT approach, together with the Schrödinger equation including relativistic kinematics.[8] The phenomenological fits indicated by the dashed curves in Fig. 1 result from the Woods-Saxon potential parameters which in the usual notation[9] $V$, $V_{s.o.}$, $W_{s.o.}$ and $r_0, a_0, r_I, a_I, r_{s.o.}, a_{s.o.}, r_c$ are given by −3.49, 78.7, 0.702, and 2.34 MeV and 0.985, 0.454, 0.940, 0.587, 1.005, 0.511, and 1.05 fm, respectively.

The KMT analysis, also shown in Fig. 1 utilized point-proton densities extracted from the $^{16}$O charge density of Sick and McCarthy,[10] including the neutron electric form factor.[11] Local approximations for the generally nonlocal second-order terms in the optical potential due to the Pauli, short-range dynamical, and center-of-mass correlations have been included as prescribed by Harrington and Varma[5] and by Schaeffer.[3,12] The effect of these terms (proportional to the square of the nuclear density) is to increase the magnitude of the differential cross section by about 20% (35%) at the second (third) maximum. Similar effects have been observed in analyses of 1-GeV $^{16}$O$(p,p)$ data when correlations were included in KMT[3]- and Glauber-model[13] calculations. The spin-independent nucleon-nucleon ($N$-$N$) amplitudes were taken from Ref. 4, while the spin-dependent amplitudes and the neutron point-density distribution were varied to optimize the fit to both the cross section and analyzing power. The resulting values for the isospin-averaged, spin-dependent parameters (defined in Ref. 4) are $\bar{\theta}_p = 14.4$ fm$^2$, $\bar{\alpha}_{sp} = 0.49$, and $\bar{B}_{sp} = 0.2$ fm$^2$, and the resulting neutron rms radius is 2.66 fm, compared to the empirical proton rms radius of 2.612 fm.

Uncertainties in the neutron rms radius due to errors in the cross-section normalization, scattering angle, charge density, beam energy, and $N$-$N$ amplitudes have been estimated. Contributions from statistical errors in the data, ambiguities in the model, and errors in the approximations used to calculate the second-order potential terms have also been estimated. The resulting uncertainty in $\langle r_n^2 \rangle^{1/2}$ is ±0.2 fm. The largest contributors to this error are ambiguities in the empirically determined spin-dependent amplitudes, and the cross-section normalization error. Calculations using equal proton and neutron density distributions [$\rho_n(r) \equiv \rho_p(r)$] are not significantly different from those displayed in Fig. 1. Hence our results are consistent with $\rho_n(r) = \rho_p(r)$.

Distorted-wave impulse-approximation (DWIA) calculations have been performed for the $^{16}$O inelastic transitions leading to the $1^-$, $2^+$, and $3^-$ normal-parity excitations. For convenience, the distorted waves were generated with the phenomenological optical potential whose parameters are given above. The transition densities were chosen to fit published $(e,e')$ data.[14] This prescription removes most uncertainties due to nuclear structure; so the calculations test the one-step reaction mechanism and the applicability of the impulse approximation, and provide an additional measure of the validity of the $N$-$N$ amplitudes. In the present calculations, the $N$-$N$ amplitudes resulting from the KMT analysis of the elastic scattering data were used, and the point-neutron transition densities were assumed to be equal to the proton ones.

The functional form assumed for the transition densities is that suggested by the harmonic-oscillator shell model, namely

$$\rho_{tr}(r) = \sum_n C_n \alpha^{n+3} r^n e^{-\alpha^2 r^2}. \quad (1)$$

The parameters obtained by fitting the longitudinal electron scattering form factors of Ref. 14 are given in Table I. The shape of the transition density for the $3^-$ excitation, i.e., $n = 3$ in Eq. (1), is just that which would be obtained in a $1\hbar\omega$ particle-hole calculation. This is sufficient to pro-

TABLE I. Point-proton transition-density prameters.

| $J^\pi$ | $\alpha$ (fm$^{-1}$) | $C_1$ | $C_2$ | $C_3$ | $C_4$ |
|---|---|---|---|---|---|
| $1^-$ | 0.527 | 1.210 | | − 0.487 | |
| $2^+$ | 0.515 | | − 0.0856 | | 0.172 |
| $3^-$ | 0.554 | | | 0.516 | |

vide an excellent fit to the electron scattering data over the momentum-transfer range $q = 0$–$3.0$ fm$^{-1}$. The value of the size parameter, $\alpha = 0.554$ fm$^{-1}$, is quite close to that inferred for the spherical part of the ground state in a two-component (spherical and deformed) treatment of the form factors for elastic electron scattering and the $0^+$(g.s.) → $0^+$(6.05 MeV) transition.[15] This is consistent with the expectation that the $3^-$ level is a vibration built on the dominant spherical component of the ground state. The shape of the transition density for the $1^-$ excitation, i.e., $n = 1$ and $n = 3$ in Eq. (1) with $C_1/C_3 = \frac{5}{2}$, is also consistent with a $1\hbar\omega$ particle-hole calculation with spurious center-of-mass motion projected out. The electron scattering data are not as complete here as in the $3^-$ case, covering only the range $q = 0$–$1.7$ fm$^{-1}$; however, the data clearly favor a size parameter for the $0^+$(g.s.) → $1^-$ transition that is smaller than that of the spherical component of the ground state. This suggests that this transition may be more complicated than a simple vibration about a spherical shape. The transition density for the $2^+$ excitation is consistent with a rotational excitation built on the deformed component of the ground state. This is clearly reflected in the small size parameter, $\alpha = 0.515$ fm$^{-1}$, which is just that obtained for the deformed component of the ground state in the analysis of the elastic data and the inelastic data for the $0^+$ → $0^+$ transition.

The $N$-$N$ amplitudes used in the DWIA calculations were the same as those used in the elastic scattering analysis. The results of these calculations are shown in Fig. 2. The overall agreement between the DWIA results and the data is rather good, particularly for the $2^+$ and $3^-$ excitations. The measured asymmetries, particularly at small angles, and the large-angle cross sections are quite sensitive to the spin-orbit amplitudes. This is clear from a comparison of the results with and without the spin-orbit amplitudes included. The main feature of the differential cross section for the $1^-$ excitation is that it peaks at an angle greater than is characteristic for orbital angular momentum transfer ($L = 1$) to the target. This effect, which is due to the suppression of the low-momentum components of the transition density that occurs when the spurious center-of-mass motion is removed, is reasonably reproduced by the theoretical calculation. The experimental analyzing power for this transition

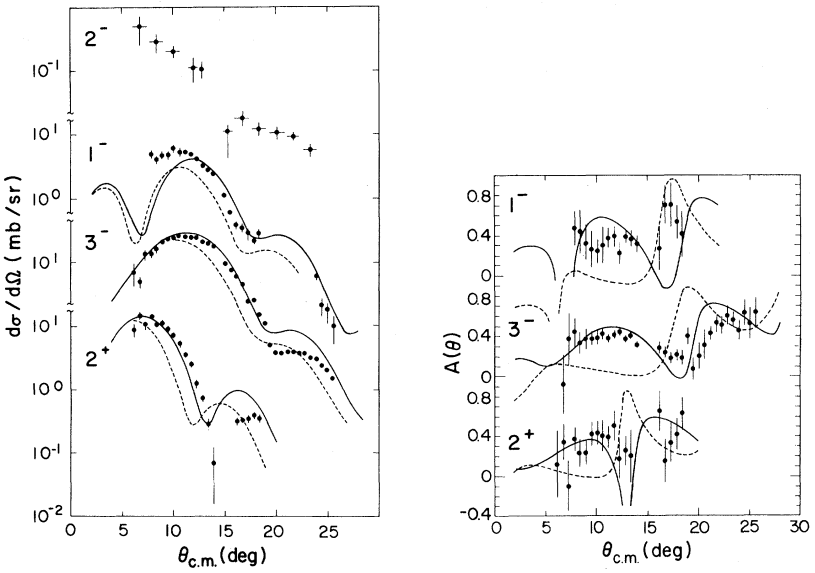


FIG. 2. Differential cross sections and analyzing powers for the low-lying excited states in $^{16}$O compared with DWIA calculations: solid line with $\vec{L}\cdot\vec{S}$, dashed line without $\vec{L}\cdot\vec{S}$. The unresolved $0^+$(6.05 MeV) contribution to the $3^-$ data is predicted to be negligibly small. The same spin-dependent optical potential was used for all calculations.

is not well reproduced by the theoretical calculation. This difficulty may be due to the neglect of amplitudes in the calculation corresponding to spin angular momentum transfer ($S=1$) to the target. Although these amplitudes are generally small for natural-parity transitions,[16] they may be important for $1^-$, $T=0$ excitations because of the suppression of the low-$q$ components in the $S=0$ amplitude. This currently being investigated using a $1\hbar\omega$ particle-hole model. Experimental data on the transverse electron scattering form factor for this transition would be useful here.

No calculations have been made for the transition to the $2^-$, $T=0$ unnatural-parity state in $^{16}$O. Analysis of this transition is complicated by the fact that very little is known about the spin-spin parts of the $N$-$N$ $t$ matrix at 800 MeV. Also, $(e,e')$ form factors do not exist for this state and so one must rely on model wave functions to calculate the transition density. Calculations for this transition will be presented in a later paper.

In conclusion, the KMT analysis of the $^{16}$O$(\vec{p},p)$ reaction is in good agreement with the elastic-cross-section and analyzing-power data. The deduced neutron density is found to be insignificantly different from the proton density. A more refined investigation of $\rho_n(r)$ would require better estimates of the second-order optical-potential terms and less uncertainty in the spin-orbit parameters. The DWIA calculations for the natural-parity inelastic transition are also found to give a good description of the experiment. The spin-orbit amplitudes are quite important for the forward-angle inelastic analyzing powers.

This work was supported by the U. S. Department of Energy, the National Science Foundation, and the Robert A. Welch Foundation.

---

[a]Present address: Centre d'Etudes Nucléaires de Saclay, Gif-sur-Yvette, France.

[b]Present address: Physics Department, University of California, Los Angeles, Cal. 90024.

[1]A. K. Kerman *et al.*, Ann. Phys. (N.Y.) 8, 551 (1959).

[2]G. Igo, Rev. Mod. Phys. 50, 523 (1978); J. Saudinos and C. Wilkin, Annu. Rev. Nucl. Sci. 24, 341 (1974), and references therein.

[3]A. Chaumeaux, V. Layly, and R. Schaeffer, Ann. Phys. (N.Y.) 116, 247 (1978).

[4]L. Ray, W. R. Coker, and G. W. Hoffmann, Phys. Rev. C 18, 2641 (1978), and references therein.

[5]D. R. Harrington and G. K. Varma, Nucl. Phys. A306, 477 (1978).

[6]H. B. Willard *et al.*, Phys. Rev. C 14, 1545 (1976).

[7]G. W. Hoffmann *et al.*, Phys. Rev. Lett. 40, 1256 (1978).

[8]W. R. Coker, L. Ray, and G. W. Hoffmann, Phys. Lett. 64B, 403 (1976).

[9]C. M. Perey and J. G. Perey, At. Data Nucl. Data Tables 13, 293 (1974).

[10]I. Sick and J. S. McCarthy, Nucl. Phys. A150, 631 (1970).

[11]W. Bertozzi *et al.*, Phys. Lett. 41B, 408 (1972).

[12]V. Layly and R. Schaeffer, Phys. Rev. C 17, 1145 (1978).

[13]E. Bleszynska, Ph.D. thesis, Jagiellonian University, 1977 (unplished).

[14]H. Miska *et al.*, Phys. Lett. 59B, 441 (1975); J. C. Bergstrom *et al.*, Phys. Rev. Lett. 24, 152 (1970); Y. Torizuka *et al.*, Phys. Rev. Lett. 22, 544 (1969); Hall Crannel, Phys. Rev. 148, 1107 (1966); G. R. Bishop *et al.*, Nucl. Phys. 53, 366 (1964).

[15]F. Petrovich, unpublished.

[16]F. Petrovich *et al.*, Phys. Rev. C 16, 839 (1977).